



## Projection of future glacier and runoff change in Himalayan headwater Beas basin by using a coupled glacier and hydrological model

Lu Li<sup>1</sup>, Yukun Hou<sup>3</sup>, Chong-Yu Xu<sup>2</sup>, Hua Chen<sup>3</sup>, Sharad K Jain<sup>4</sup>

5 <sup>1</sup>Uni Research Climate, Bjerknes Centre for Climate Research, Jahnebakken 5, 5007 Bergen

<sup>2</sup>Department of Geosciences, University of Oslo, Norway

<sup>3</sup>Wuhan University, Wuhan, China

<sup>4</sup>National Institute of Hydrology, Roorkee, India

*Correspondence to:* Lu Li (lu.li@uni.no)

10 **Abstract.** The Himalayan Mountains are the source region of one of the world's largest supplies of freshwater. The changes in glacier melt may lead to droughts as well as extreme rains and floods in the Himalaya basins, which are vulnerable to the hydrological impacts. This study used a glacio-hydrological model: Glacier and Snow Melt - WASMOD model (GSM-WASMOD) for the hydrological projections under 21st century climate change by two RCMs under two Representative Concentration Pathways (RCP4.5 and RCP 8.5) in order to assess the future water change at the Himalayan Beas basin. In  
15 addition, the glacier extent loss of the 21st Century from eight GCMs was also investigated as part of the glacio-hydrological modelling as an ensemble simulation.

The glacio-hydrological modeling shows that at present, the annual glacier imbalance accounts for about 14% of the total runoff in this area. Under Climate change impact, the temperature will increase 0.95 °C (RCP4.5) and 1.67 °C (RCP8.5) for the early future (2046-2055), and increase 1.53 °C (RCP4.5) and 3.4°C (RCP8.5) for the late future (2090-2099). The glacier  
20 area loss is about 47 % (RCP4.5) and 49 % (RCP8.5) for the early future and 73 % (RCP4.5) and 80 % (RCP8.5) for the late future. This will result in a decrease in river runoff in general for all the scenarios. The heaviest decrease of Beas river runoff can be observed in August under RCP4.5 and in May under the RCP8.5 for both the near future and far future. This maximum decrease of river runoff also has the largest spread. Furthermore, a high resolution WRF precipitation suggested a much heavier winter precipitation over high altitude area in the Himalaya Beas river basin. The study helps to understand the  
25 hydrological impacts of climate change in North India and make a contribution to stakeholders and policy makers with respect to the future of water resources in North India.

### 1 INTRODUCTION

The changes in glacier melt may lead to droughts and floods in the Himalayan basins, which are one of the world's largest supplies of freshwater. Hydrological models have been developed and used as a main assessment tool in Himalaya region to  
30 estimate present and future water resources for purposes of climate change impact. However, most hydrological models either don't have glacier representation (Ali et al., 2015; Horton et al., 2006; Stahl et al., 2008) or don't have proper glacier representation with limited glacier cover assumption (i.e. intact-, 50% or no-glacier) (Akhtar et al., 2008; Hasson 2016; Aggarwal et al. 2016). A glacio-hydrological model which includes a comprehensive parameterization of glaciers is highly required for the water resources assessment of high mountainous basins over Himalayan region. Recently, Lutz et al. (2016)  
35 investigated the future hydrology by a glacio-hydrological model with proper representative glacier module over the whole mountainous Upper Indus Basin (UIB) with the ensemble of statistically downscaled CMPI5 GCM. Results obtained by them indicated a shift from summer peak flow towards the other seasons for the most ensembles and large uncertainty in monsoon influence and importance of meltwater. More intensity and frequency of extreme discharge are likely to occur for UIB in the future of the 21st century by their study. Besides, Li et al. (2016) applied a hydro-glacial model at two basins in



40 Himalaya region and assessed the future water resources under climate change scenarios, which were generated by two bias  
corrected COordinated Regional climate Downscaling EXperiment (CORDEX, Jacob et al. 2014) data from the world  
Climate Research Program (WCRP). However, their results showed a conflicting future glacier cover at the end of the  
century under different scenarios. Especially in Beas river basin, the result indicated that the glaciers are predicted to gain  
45 mass under RCP2.6 and RCP4.5 while lose mass under RCP8.5 for the late future after 2060. This conflicting future is not  
only seen for the glacier projections but also for the river flow. The impact of glacier melt on river flow is noteworthy,  
although the precipitation is generally predicted to be increasing in the future in the Himalaya region. On the one hand, some  
studies suggested an increase of future water availability in Upper Indus Basin over Himalayan region for the 21st century  
(Ali et al., 2015; Lutz et al., 2014; Khan et al., 2015). On the other hand, a substantial drop in the glacier melt and  
subsequently reduction in water availability is suggested for the near future by the other studies (e.g. Hasson, 2016).  
50 Furthermore, a few recent studies suggested highly uncertain water availability in the late/long-term future and no consistent  
conclusion can be seen in the UIB over Himalaya region (e.g. Lutz et al., 2016). As of now, there is a lack of in-depth  
understanding of the water resources in the future, which will be highly affected by glacier melting in the mountainous basin  
over Himalaya region (Hasson et al., 2014; Li et al., 2016; Lutz et al., 2016; Ali et al., 2015).

In order to investigate the climate change impact on the future water availability, the RCMs are used to downscale the  
55 variables produced by GCMs for use as the inputs to hydrological models. This approach is adopted because the outputs of  
GCMs are too coarse to use directly as input for hydrological model at regional or basin scale (Akhtar et al., 2008).  
However, the RCM simulations still have systematic biases resulting from imperfect physical processes, numerical  
approximations and other assumptions (Eden et al., 2014; Fujihara et al., 2008; Anand et al. 2017). In this case, most of the  
studies applied bias correction based on RCM simulations as input for hydrological models (Troin et al., 2015; Johnson and  
60 Sharma, 2015; Li et al., 2016; Ali et al., 2014; Teutschbein and Seibert, 2012). However, this bias correction results in  
physical inconsistencies since the corrected variables are not independent of each other (e.g. Immerzeel et al., 2013). For  
instance, although bias corrected RCM precipitation data will improve the hydrological calibration results, it will no longer  
be consistent with modeled other variables, e.g. temperature, radiation. It is generally based on the assumption of stationary  
climate distribution in terms of the variance and skewness of the distribution, which however is crucial for assessing the  
65 impact of climate change on seasonality and extremes of hydrological cycle. Furthermore, some recent studies have  
evaluated CORDEX data and have highlighted the need for proper evaluation before use RCMs for impact assessment for  
sustainable climate change adaptation. For instance, Mishara (2015) analyzed the uncertainty of CORDEX and the results  
showed that the RCMs exhibit large uncertainties in temperature and precipitation in south Asia regional model and are  
unable to reproduce observed warming trends. Singh et al. (2017) compared CORDEX with GCMs and found that no  
70 consistent added value is observed in the RCM simulations of changes in Indian Summer Monsoon Rainfall over the recent  
periods in general. In this case, statistical downscaling method is chosen as it might be better suited to the Himalayan  
headwater river basin with very complex topography.

At present, a complete understanding of the hydroclimate variability is also a challenge in the Himalayan basins due to poor  
in-situ coverage (Maussion et al., 2011) and incomplete or unreliable records (Hewitt 2005; Bolch et al. 2012; Hartmann and  
75 Andresky 2013). Besides, precipitation in the Himalayan region is strongly influenced by terrain. The regional patterns and  
amounts of the precipitation are not always captured by global gridded precipitation datasets (e.g. Tropical Rainfall  
Measuring Mission (TRMM) (Huffman et al. 2007), ERA-Interim (ECWMF, Dee et al., 2011), Climate Research Unit (CRU)  
(Mitchell and Jones, 2005), and the Asian Precipitation - Highly-Resolved Observational Data Integration Towards  
Evaluation (APHRODITE) (Yatagai et al. 2012) (see also Biskop et al. 2012; Dimri et al. 2013; Ménégoz et al. 2013; Ji and  
80 Kang 2013). Previous studies showed that the high-resolution (<4km grid spacing) RCMs have demonstrated reasonable  
skill in reproducing precipitation distribution and intensity patterns over complex terrain (e.g., Rasmussen et al. 2011, 2014;  
Collier et al. 2013).



A high-resolution Weather Research and Forecasting (WRF) dynamical simulations has been applied in the Beas basin in Himalaya showing promising potential in addressing the issue of high spatial variability in the complex terrain and high elevation precipitation (Li et al., 2017). This high-resolution WRF model provides a first estimation of liquid and solid precipitation in high altitude areas, where satellite and rain gauge networks are not reliable. Due to the underestimation of summer precipitation in WRF at the foothill of the basin in its western part, we combined this high-resolution WRF data with gauge data. A solid understanding of the water cycle in the Himalaya headwater basin is interpreted in this study. The comparison of the simulations from gauge precipitation, WRF precipitation and the combined precipitation is further assessed. There is a large uncertainty of winter precipitation over high altitude area in Himalayan river basin. In this study, a glacio-hydrological model has been applied in the Beas river basin in Himalaya for assessing the current and future water resources by two statistical downscaling methods under climate change scenarios. An ensemble of glacier cover changes over 21st century are included and investigated in the future water projections under climate change impact. In addition, the measured annual mass balance was used together with discharge data for the glacio-hydrological model calibration in Beas river basin. The main questions whose answer we are seeking in this study are: (1) how will the future water availability change due to higher glacier melt under warmer future in Beas river basin over the Himalaya region? (2) How will the hydrological seasonality change in the Beas river basin in future? (3) How much precipitation falls at the ungauged high altitude area in the Beas river basin?

After the introduction of section 1, we present details of the study area and data in section 2. In section 3 on methodology, we describe the glacio-hydrological model, glacier evolution method, statistical downscaling (SD) methods and model calibration. In section 4, we focus on the simulation of the present day water cycle and validation of the simulated discharge by using the observed discharge. Besides, the future climate change and glacier extent change and hydrological changes will be investigated here. Finally, the experiment simulation of combined precipitation from WRF and gauge data is studied and the uncertainties of the hydrological simulation in the study has been discussed in section 5, before presenting the main conclusions in section 6.

## 2 STUDY AREA AND DATA

### 2.1 Study area

The study area is Beas river basin upstream of the Pandoh Dam with a drainage area of 5406 km<sup>2</sup>, out of which only 780 km<sup>2</sup> is under permanent snow and ice. It is one of the important rivers of the Indus River system. The length of the Beas River up to Pandoh is 116 km; among its tributaries Parbati and Sainj Khad Rivers are glacier fed. The altitude of the study area varies from about 600 m to above 5400 m. The study area falls in lower Himalayan zone and varies in climate due to elevation difference. The mean annual precipitation is 1217 mm, of which 70% occurs in the monsoon season from July to September. The mean annual runoff is 200 m<sup>3</sup>/s, of which 55% occurs in the monsoon season and only 7.2% occurs in the winter from January to March (Kumar et al., 2007). The mean temperature rises above 20°C in the summer and falls below 2°C in the January. The model was calibrated against observed discharges at the watershed outlet (Thalout station). The hydrological and metrological data from 1990 to 2004 have been used in the study. These data have undergone quality control in the previous studies (Kumar et al., 2007, Li et al., 2013a, 2015a). The topography and drainage map of the river system along with rain gauge stations is shown in Fig. 1.

### 2.2 Data

This study used HYDRO1k to delineate the basin boundaries. HYDRO1k is derived from the GTOPO30 30-arc-second global-elevation dataset (USGS) and has a spatial resolution of 1 km. HYDRO1k is hydrographically corrected such that local depressions are removed and basin boundaries are consistent with topographic maps. Daily precipitation of 7 rain gauge



stations, daily minimum and maximum temperature of 4 meteorological stations and daily potential evapotranspiration of one station are obtained from Bhakra Beas Management Board (BBMB) in India were used for GSM-WASMOD modelling. The outlet discharge station of Thailout was used for GSM-WASMOD model calibration and evaluation, which was also obtained from the BBMB. Furthermore, the daily precipitation from a horizontal 3 km WRF simulation by Li et al. (2017) is also used in the study for further experiment and discussion on the precipitation uncertainty.

### 3 METHODOLOGY

#### 3.1 Glacier- and snow- melt module (GSM)

A conceptual glacier- and snow- melt module (GSM) was used to compute glacier mass balances and melt-water runoff from the glacier in the study basin, which was only applied to the grid cells of the glacier-covered area. Those glacier grid cells were defined by ESRI ArcGIS system v. 9.0 (or higher) and set up before modeling based on the Global Land Ice Measurements from Space (GLIMS) Glacier Database (<http://glims.colorado.edu/glacierdata/glacierdata.php>) (Berthier, 2006; Raup et al., 2007; Li et al., 2013a). The daily temperature and precipitation were input data for the GSM module, which calculated both snow accumulation and melt-water runoff. In the GSM module simulation, the precipitation shifted from rain to snow linearly within a temperature interval of  $\Delta T$  (Table 1). In the study, the 1<sup>st</sup> of October was assumed to be the time when the snow (which has not melted away during summer) transferred to be firn. Besides, 20 % of the existing firn was assumed to become ice. In this case, an average transition time from firn to ice was five years. Additionally, the liquid water in the snow from rain or melt infiltrated and refreeze in the snowpack, which filled the available storage. Runoff occurred when the storage was filled, which depended on the snow depth. The snow started melting firstly, which followed by the melting of the refrozen water and firn accordingly. At the last, the (glacier) ice started to melt when the firn has all melted away. We used a degree-day-factor of firn ( $DDF_f$ ) and ice ( $DDF_i$ ), which are 15 % and 30 % larger than that of snow ( $DDF_s$ ), respectively. A temperature-index approach (Hock 2003; Engelhardt et al. 2012, 2017) was used in the study for the calculation of the conceptual GSM module. The related equations can be found in Table 1.

#### 3.2 GSM-WASMOD model

A glacio-hydrological model: Glacier and Snow Melt - WASMOD model (GSM-WASMOD) was developed in the study by coupling the macro scale water and snow balance modeling system (WASMOD-D) (Xu, 2002; Widen-Nilsson et al., 2009; Gong et al., 2009; Li et al., 2013b, 2015b) with the GSM module. The spatial resolution of the GSM-WASMOD modeling is 10 km in the study. The daily precipitation, temperature and potential evapotranspiration from the observed stations were interpolated by Inverse Distance Weighted (IDW) method to be 10 km resolution gridded data, which were used as input for the GSM-WASMOD model. It calculates snow accumulation, snowmelt, actual evapotranspiration (ET), soil moisture, fast flow and slow flow at the non-glacier area. The routing process of GSM-WASMOD model in the study is the aggregated network-response-function (NRF) routing algorithm, which was developed by Gong et al. (2009). The spatially distributed time-delay was calculated and preserved by the NRF method based on the 1 km HYDRO1k flow network, which is from U.S. Geological Survey (USGS). The runoff generated in the lower resolution of 10 km grid, whose delay dynamics were transferred by the NRF method based on the simple cell-response function. More details can be found in Gong et al. (2009). The equations of GSM-WASMOD model are shown in Table 1.

#### 3.3 Glacier evolution ensemble

GSM-WASMOD is a large-scale conceptual glacio-hydrological model, which means that the glacier extent is not changing in the historical simulation. This assumption has to be changed in future simulation under climate change, since the future of the glacier extent is a crucial factor for the future hydrology in the Beas river basin. In this case, we used the glacier evolution result





from a parameterization of glacier mass balance model (Lutz et al., 2016). It forces a regionalized glacier mass balance model for Upper Indus Basin (UIB) and estimates changes in the glacier extent as a function of the glacier size distribution and temperature and precipitation. The glacier changes are the result of a close interplay of projected changes in temperature and precipitation, which are calculated monthly in the parameterization approach. In the method, the seasonal timing of the projected temperature and precipitation projections is very important because changes can apply to the ablation season (summer) or the accumulation season (Winter). In the glacier evolution, totally eight ensemble model runs were applied including two Representative Concentration Pathways (RCPs) (RCP4.5 and RCP8.5) with four GCMs (see Table 2). More details can be found from (Lutz et al., 2014).

### 3.4 Statistic downscaling

The downscaling techniques are used to link large-scale atmospheric variables to smaller-scale meteorological variables for driving the hydrological model, since GCM is spatially too coarse to determine the regional and basin scale effects of climate change (Rudd and Kay 2016). In this study, two regression-based statistical downscaling methods, i.e. Statistical Downscaling Model (SDSM) (Wilby et al. 2002; Chen et al. 2012) and Smooth Support Vector Machine (SSVM) (Chen et al. 2010, 2012), were applied for downscaling of the daily precipitation, maximum daily temperature (tmax), minimum daily temperature (tmin) and daily evapotranspiration in a Himalayan head water basin under climate change of the 21st Century.

#### 3.4.1 Statistical Downscaling Model (SDSM)

The SDSM method was proposed by Wilby et al. (2002), which is a decision support tool for estimating climate change impacts and has been widely used in the climate change studies (Wilby and Dawson 2013; Dibike 2005; Chu et al. 2010; Tatsumi et al. 2014). SDSM is a classic and popular method of statistical downscaling (Koukidis and Berg, 2009). It implements linear regression (MLR) to estimate the amount and/or the occurrence of local meteorological predictands. SDSM behave well in keeping mean of predictands, while it is weak in simulating standard deviation and extreme values (Hessami et al., 2008). For precipitation, the SDSM firstly reproduces the occurrence of precipitation, just like Weather Generator, before the magnitude simulation. The occurrence generator of SDSM in conditional downscaling is based on the regression of predictor variables:

$$W_t^{sim} = a_0 + \sum_{i=1}^j a_i \hat{u}_t^i$$

$$w_t^{sim} = \begin{cases} 1 & rand \leq W_t^{sim} \\ 0 & rand > W_t^{sim} \end{cases} \quad (1)$$

where  $a_0$  is an underlying probability and  $a_i$  is the weight of the  $i$ th predictor. The magnitude generator is the MLR algorithm, which is commonly used in regression-based methods. The advantages of SDSM are the superior ability of simulation and the visual, user-friendly interface that does not exist in most of the downscaling models. The latest SDSM software (version 5.1) strengthens the ability for creating more complex transformations of the input series.

#### 3.4.2 Smooth Support Vector Machine (SSVM)

The Support vector machine (SVM) is a learning method based on the Vapnik-Chernonenkis (VC) dimension and structural risk minimization (SRM) (Vapnik 1998). It overcomes the problem of local extreme, which can be often found in other learning method. In this case, SVM can better deal with the small sample, nonlinear, high dimension and local minimum points and other practical issues, which makes SSVM ideal performance in regressing the precipitation with atmospheric variables.



195 SVM assumes that there is a training set  $\{X_i, Y_i\}_{i=1}^l$ , where  $X$  represents a multidimensional input vector and  $Y$  is an output vector. Firstly, a function  $\phi(X)$  is utilized to translate  $X$  from the original space into high-dimension space, in which an optimal decision function is constructed:

$$Y = W^T \cdot \phi(X) + b \quad (2)$$

where  $W$  and  $b$  are the parameters. Aiming at minimizing the structural risk, an objective function  $R$  is constructed as:

200 
$$R = \min \left\{ \frac{1}{2} \|W\|^2 + C \sum_{i=1}^l \xi_i^2 \right\} \quad (3)$$

In which,  $\xi$  is the loss function and  $C$  is the regularization parameter. Besides, a kernel function  $K(X_i, X_j)$  which meets the Mercer condition  $F$  is a way to handle input vector such that:

$$K(X_i, X_j) = F(\phi(X_j), \phi(X_i)) \quad (4)$$

After the model optimization, finally the determined decision function  $f(X_i)$  can be written as:

205 
$$f(X_i) = \sum_{i=1}^l \alpha_i K(X_i, X_j) + b \quad (5)$$

where  $\alpha_i$  is the Lagrange multiplier. The calculation of SVM costs a relatively large demand for computation, since the objective function of initial SVM is not strictly constrained. Therefore, a smoothing technique is utilized in SSVM to make the algorithm converges to the unique solution in order to have a better efficiency than SVM (Lee and Mangasarian, 2001). In this study, SSVM is directly used to construct the relationship between hydrological data and atmospheric variables in order to simulate future climate change by this relationship.

210 Both of the above statistical downscaling models are calibrated in the historical period of 1979-2005 for precipitation, 1985-2005 for minimum and maximum temperature, and 1996-2005 potential evapotranspiration for each month. The calibration of downscaling models used the station-scale hydrological data and GCM historical atmospheric variables to construct the relationship. The calibrated downscaling models are then utilized to predict the future climate change with the GCM variables from 2006 to 2099 in the RCP4.5 and RCP8.5 scenario.

### 3.5 Model calibration

There are six parameters to be calibrated in GSM-WASMOD by searching for an optimal parameter set for the discharge station at Thalout, including the snowfall temperature  $a_1$ , snowmelt temperature  $a_2$ , actual evapotranspiration parameter  $a_4$ , the fast-runoff parameter  $c_1$ , the slow-runoff parameter  $c_2$  and the degree-day factor of snow  $DDF_s$ . The average annual glacier mass balance and discharge station in Beas River basin are both used for the calibration in the study (Li et al. 2013; Azam et al. 2014). The calibration and validation time period used for this study were 1990-2000 and 2001-2004, respectively. We used the data of 1990 for three preceding spin-up years. GSM-WASMOD run with the 5000 parameter sets, which were obtained by the Latin-Hypercube sampling method (Gong et al., 2009, 2011; Li et al., 2015a). The best parameter set was then chosen based on three indices, including Nash-Sutcliffe coefficient (NSC) (Nash and Sutcliffe, 1970), relative volume error (VE) and root-mean-square error (RMSE). For the best model performance, the NSC is to be 1 and the other two indices, i.e. VE and RMSE, are to be 0.



## 4 RESULTS AND DISCUSSIONS

### 4.1 GSM-WASMOD calibration and validation

The calibration (1990-2000) and validation (2001-2004) results from WASMOD and GSM-WASMOD are given in Table 3, which shows that GSM-WASMOD has obviously improved the performance of WASMOD in reproducing historical discharge in Beas river basin. For the calibration of GSM-WASMOD, the monthly NSC and daily NSC are 0.74 and 0.66 respectively. The RMSE and VE are 1.4 and 9%, respectively. For the Beas river basin, located to the North mountainous India, the model underestimates the flow during June-August, which leads to a large negative bias (Fig. 2). The mean annual precipitation is 1237 mm/yr for 1990-2004, while the observed discharge is even higher which is 1267 mm/yr. Comparing the observed discharge and precipitation, the bias is most likely related to an underestimation of precipitation due to limited rain gauge stations. More detailed components of simulated flow are shown in Fig. 3.

In Beas river basin, the Chhota Shigri glacier is the main glacier, which is close to Bhuntar. The total runoff (including rainfall discharge, ice- and snow-melt discharge) from glacier cover area contribute about 24 % of total runoff and the glacier imbalance is about 14 % of total runoff in Beas River basin up to Thalout station during 1990-2004. The monthly hydrography of ice and snow melt discharge, total glacier area discharge, and simulated and observed discharges during the calibration and validation period are shown in Fig. 4. Besides, the daily observed and simulated discharge series and snow and ice-melt runoff at 1999 are shown in Fig. 5 for illustrative purpose, which reveals that the GSM-WASMOD worked fine in the study basin for reproducing the historical discharge. The annual glacier mass balance of Beas river is -1.0 m/a w.e. of 1990-2004 and -1.2 m/a w.e. of 1999-2004 in the study (Fig. 6), which is comparable to the measured values from the previous studies, i.e. the measured annual glacier mass balance (1999-2004) of Chhota Shigri glacier is -1.02 or -1.12 m/a w.e. by Berthier et al. (2007) and -1.03(+/- 0.44) by Vincent et al. (2013). Considering the uncertainties in the meteorological forcing data and high complexity in the hydrological cycle over high altitude Himalaya mountainous area, the model is considered to be satisfactory for estimating the impacts of climate change for the Beas's water future.

### 4.2 Future climate change

The climate change scenarios for GSM-WASMOD simulation are illustrated in Table 4. Fig. 7 and Fig. 8 show the changes of precipitation and temperature of the Beas river basin in the early future (2046-2055) and the late future (2090-2099) compared with the baseline period (2006-2015). The temperature in monsoon season from both SDSM and SVM will increase; there is more uncertainty in winter. The SDSM shows slight decrease of temperature during November to January, which is not seen in SVM scenarios.

The ten-yrs moving averages of annual precipitation and temperature of the Beas river basin are shown in Fig. 9. From the Figure, we can see that under Climate change impact, the study area will be getting warmer in all scenarios in the study. A more detailed statistical analysis result is shown in Table 5. The annual mean temperature of Beas river basin are approximately warm up to  $\sim 0.95$  °C (RCP4.5) and  $\sim 1.67$  °C (RCP8.5) in the middle of the century (2046-2055) comparing with baseline period (2006-2015), and up to  $\sim 1.53$  °C (RCP4.5) and  $\sim 3.5$  °C (RCP8.5) at the end of the century (2090-2099) comparing with the same baseline period. For the annual mean precipitation, the change will be +5 % (RCP4.5) and +16.6 % (RCP8.5) in the middle of the century (2046-2055) comparing with the baseline period (1990-2000), and +6 % (RCP4.5) and +26.9 % (RCP8.5) in Beas river basin at the end of the century (2090-2099). However, there is larger precipitation increase from SDSM scenarios than that from SVM. In general, the Beas river basin will get warmer and wetter compared to the historical period, which are confirmed by other studies (e.g. Aggarwal et al. 2016; Ali et al. 2015). Under SDSM RCP8.5, the temperature increases the most, while for precipitation, the SVM RCP8.5 increases the most.



#### 4.3 Future glacier extent change

The glacier evolutions in Beas river basin under eight climate change scenarios are shown in Fig. 10. The glacier extent will keep retreating in the future at Beas river basin. There are large uncertainties in the changes of the glacier extent from different projections (Fig. 10), which confirmed by the other studies (e.g. Lutz et al., 2016; Li et al. 2016). In this study, the glacier extent scenarios are from the study of Lutz et al. (2016), from which the decreases of glacier extent over Beas river basin are approximately ~ 42 % (RCP4.5) and ~ 46 % (RCP8.5) in the middle of the century (2050) and ~ 72 % (RCP4.5) and ~ 87 % (RCP8.5) at the end of the century (2100) compared with the baseline year of 2000. For instance, the decrease of glacier extent varies from 40% to 90% between different projected scenarios at the end of the century. One of the main factors leading to the large spread of glacier extent projections between the models is the large uncertainty in future precipitation, which feeds the glaciers (Lutz et al., 2016). The spatial distributions of the glacier extent of Beas river basin at present, in the middle of the century and at the end of the century under RCP4.5 and RCP8.5 are shown in Fig. 11. It suggested that the glacier area decreases considerably in the 21st century in Beas river basin. This is most likely because of the ample rise in temperature, although the precipitation increases as well.

#### 4.4 Future Hydrological changes

There is a consistent trend of projected hydrological changes over all the scenarios, although there are large uncertainties in the future climate and future glacier extent change. The runoff is projected to decrease by the end of the century across all the scenarios (Fig. 12). Table 5 shows the change of glacier extent, precipitation, temperature, discharge and Evaporation (ET) in Beas river basin in the middle of the century (2046-2055) and at the end of the century (2090-2099) comparing with the history baseline period (2006-2015). There are large ranges in different climate change scenarios. The mean monthly future change of evapotranspiration and discharge over Beas river basin up to Pandoh are shown in Fig. 13 and Fig. 14. According to Fig. 14, the projected discharge will decrease mainly in pre-monsoon and monsoon period under both RCP4.5 and RCP8.5 for near future (2045-2055) and far future (2090-2099). Under RCP8.5, there is a slight increase from some projected discharge over winter period at the end of the century. The projected discharge shows that it will decrease more under RCP8.5 than that under RCP4.5 in general. The largest change of discharge can be observed in August under RCP4.5, which also has the widest range. The mean monthly decreases of discharge in August are round -100 mm and -140 mm for the near future and far future. For the RCP8.5, the largest decrease of discharge is in May, which is around -100 mm and -150 mm for the near future and far future. However, the most uncertain month is also August for RCP8.5, which has the widest range comparing with other months. This is probably due to the decrease of snow- and ice- melting from glacier area and the increase of temperature. It shows that the summer peak of runoff shifts to the other seasons in Beas river basin, which confirmed by the study from Lutz et al. (2016).

The percentage of glacier ablation in the total runoff in Beas river basin is projected to decrease by the end of the century over all the scenarios (Fig. 12). The projected glacier ablation is around 10 % (2.5% ~ 27%) and 6% (3% ~ 12%) of the total runoff in the middle of the century under RCP4.5 and RCP8.5, respectively. The evolution of precipitation (Pre), total discharge (Dis) and glacier ablation (Gla) from all the scenarios during 2006-2099 are shown in Fig. 12. There is a wide spreading of glacier ablation near the middle of the century, which indicates a larger uncertainty in the prediction discharge over this period.

There are several limitations of this study that need to be addressed. Firstly, only one GCM, i.e. Beijing Climate Center Climate System Model (BCC\_CSM 1.1) was used for the future forcing data of GSM-WASMOD by statistical downscaling methods in this study and four types of GCMs, including dry & cold, dry & warm, wet & cold, and wet & warm are used for glacier extent future evolution scenarios. In this case, there are wider ranges of glacier extents change than other meteorological forcing change in the future scenarios analysis in the study. A more robust projection results will probably need more GCMs for comparison. Secondly, only two statistical downscaling methods and two scenarios, i.e. RCP 45 and RCP 85, were used in the study. More ensemble RCMs are needed for predicting future river flows to include enough uncertainties. Thirdly, the spatial resolution is 10 km and for a small spatial scale basin in the study a finer resolution model will probably improve the simulated



result, especially by smoothing the glacier extent change (i.e. avoiding the step change in glacier extent evolution). In addition, the simplification of glacier module will also result in uncertainty in the results. Furthermore, the limitations of data, e.g. sparsely rainfall stations and no snowfall measurement, in such high-mountain drainage basin also lead to large uncertainty in hydrological simulation, and this is a common challenge for modeling study in this region.

## 5 DISCUSSIONS

### 5.1 Experiment: combined precipitation from gauge and WRF

According to the previous studies over Himalaya and surrounding area (Winiger et al., 2005; Immerzeel et al. 2015; Ji et al., 2015; Shrestha et al., 2012), specifically in Beas river basin up to Pandoh, there are quite large uncertainties in precipitation over high altitude area. Li et al. (2017) applied the Weather Research and Forecasting model (WRF) over Beas river basin at very high resolution of 3 km in 1996-2005. The seasonal WRF precipitation compared with gauge rainfall data is shown in Fig. 15, which indicates that the WRF model predicts more precipitation at high altitude area in Beas. Currently there are no rainfall and snowfall measurements in these areas.

In this study, we have used the data from the high-resolution WRF simulation and compared with the calibrations in the overlapping period of 1996-2003 based on gauge rainfall data and precipitation from the WRF simulation (with New Thompson microphysical scheme) by GSM-WASMOD. More details about this high resolution WRF simulation can be found in Li et al. (2017). The results show that the daily NS efficiency driving by gauged and WRF precipitations are 0.62 and 0.56, respectively. Considering that we were lacking of observed precipitation over high mountainous area in Beas river basin, especially without snowfall in winter period, we combined the gauge rainfall with the high resolution WRF data precipitation in order to provide a more reliable precipitation for the model simulation. The rules of this data combination are as follows:

1. The 3 km WRF precipitation is upscaled by arithmetic mean average to 10 km;
2. Replacement of the gauge precipitation by the upscaled WRF precipitation only applies to the grids whose altitude is over 5000 m;
3. Replacement of the gauge precipitation by the upscaled WRF precipitation only applies in winter period during December to March.

The mean annual precipitation (1996-2003) from WRF, gauge and combined precipitation are 1396 mm/yr, 1316 mm/yr and 1413 mm/yr, respectively (Fig. 16). The calibration (1996-2003) of GSM-WASMOD is done based on the combined Gauge-WRF precipitation data, from which, the daily NS efficiency of calibration is slightly higher being 0.67, comparing with 0.63 from gauge and 0.56 from WRF. The RMSE, VE and monthly NS efficiency from the calibration of GSM-WASMOD driving by the combined precipitation are 0.81, 6% and 0.75, respectively, while those by gauge precipitation are 1.0, 0.3% and 0.71, respectively. In addition, the indices of calibration result from WRF precipitation are 1.28, 8% and 0.67, respectively.

### 5.2 Uncertainty of precipitation in high altitude area

In our study, the results show a decrease in the future river flow over Beas river basin up to Pandoh in general for all future scenarios, although it varies in different seasons. The main decrease is found in pre-monsoon and monsoon period for all the scenarios, while a slightly increase can be seen in winter period at the end of the century under the scenarios of RCP8.5. The results differ from some previous studies. For instance, the future river flow in Beas river basin was projected to be increasing for the future periods (during 2006 ~ 2100) comparing with the baseline period of 1976-2005 by Ali et al. (2015). In their study, the future hydrological simulation was lacking of glacier component, which did not account for glacier retreat under future climate change impact. This might lead to overestimation of future river flow from their projections. In the other study of Li et al. (2016), large spread of river flow changes from different scenarios can be seen and no uniform conclusion can be conducted from their projections.



There are many uncertainties and challenges for the future hydrological projection under climate change in Beas river basin. In the basin, the dedication of snow and glacier melting is significant for the total runoff, which varies from 27.5 % ~ 40% by previous studies (e.g. Kumar et al. 2007; Li et al. 2013a, 2015a). In our study, the total snow and glacier melting from glacier covered area is 24% of total runoff and the glacier retreat is 14% during 1990-2004, comparing with 5% during 2003-2008 by Kääb et al. (2015), who used ICESat satellite altimetry data. There are several reasons for this large spread of percentage of snow and glacier melting in Beas river basin. Most common knowledge of one of the challenges in high mountain area is data issue. A large disagreement between precipitation from dynamical RCM simulations (WRF) and other data sources (i.e. TRMM 3B42 V7, APHRODITE and gauge data) were found over high altitude in Beas river basin by the previous study of Li et al. (2017). There are no gauge stations, which is over 2000 meters in our study and neither of the gauge stations includes appropriate snowfall measurement. Lacking of reliable snowfall measurement over the Himalaya regions is one of the reasons for a poor understanding and a large uncertain of high altitude precipitation over this area (Mair et al. 2013; Ragettli and Pellicciotti 2012; Immerzeel et al. 2013, 2015; Viste and Sorteberg 2015; Ji et al. 2015). Some studies showed that the high altitude precipitation is much larger than previously thought and other dataset (Immerzeel et al. 2015; Li et al. 2017). Comparing the high resolution WRF precipitation with gauge rainfall, the results showed underestimation of WRF at Manali station in summer period (JAS). The Manali precipitation is more heavily influenced by the complex topography than other stations, because it locates at a bit deeper valley in the mountains. This is probably the main reason that WRF underestimates the rainfall in summer period comparing with gauge rainfall. While for winter period (DJFM), the WRF results showed much larger precipitation over high altitude in Beas river basin comparing with gauge rainfall.

In the study, we made an experiment case study of GSM-WASMOD driven by the combined precipitation from gauge rainfall and the high altitude precipitation (over 5000 meters) of WRF in winter period (DJFM). We compared the GSM-WASMOD simulations from Gauge precipitation, WRF precipitation and the combined precipitation. We can also see from the results that the daily NS value from Gauge precipitation is larger than that from WRF precipitation. Furthermore, it showed an improvement of both daily NS and monthly NS efficiency from the combined precipitation over that from Gauge precipitation and WRF precipitation. This experiment result confirmed that there is probably much heavier precipitation at high altitude in Himalaya regions than what we knew from the gauge data and other gridded data set. The high-resolution precipitation of RCM, i.e. WRF has the potential for providing more information and knowledge for the high altitude precipitation in Beas river basin, which locates at the western Himalaya region, although it still has challenges in capturing accurately the spatial precipitation variability at high resolution (i.e. at complex topography such as Himalaya mountain area) and temporally (i.e. daily or hourly).

## 6 CONCLUSIONS

A glacio-hydrological model: Glacier and Snow Melt - WASMOD model (GSM-WASMOD) was applied for investigating the hydrological projection under climate change during 21st century in the Beas basin. The river flow is heavily impacted by the glacier melt. The glacier extent evolutions under climate change were conducted by Lutz et al. (2014), which were used in the study for constructing the future glacier extent scenarios for use by the GSM-WASMOD model for simulating the hydrological response of Beas river basin up to Pandoh. The changes of precipitation, temperature, runoff and evaporation in Beas river basin in the early future (2046-2055) and the late future (2090- 2099) were investigated in the project study. The results reveal that the glacier imbalance (-1.0 m/yr) is about 14 % of total runoff in Beas River basin up to Thalout station at present (1990-2004). Under Climate change impact, the temperature will increase by 0.95 °C (RCP4.5) and 1.67 °C (RCP8.5) for the early future (2046-2055), and increase 1.53 °C (RCP4.5) and 3.4°C (RCP8.5) at the late future (2090-2099), while the precipitation will increase 5 % (RCP4.5) and 16.6 % (RCP4.5) for the early future, and increase by 6 % (RCP4.5) and 26.9 % (RCP8.5) for the late future over the Beas river basin. The glacier extent loss is about 47 % under RCP4.5 scenario and 49 % under RCP8.5 scenario at the early future and 73 % under RCP4.5 scenario and 80 % under RCP8.5 scenario at the late future,





390 which results in a big loss of runoff in pre-monsoon and monsoon period.

There was a large spread of glacier extent change and runoff change in the future scenarios. The runoff was projected to decrease for the late future for all the scenarios, although the changes vary with seasons. The precipitation increase and glacier retreat make the runoff a general heavy decrease during pre-monsoon and monsoon period for all the scenarios and an even slightly increase in winter period under some projections of RCP8.5 scenario for the late future. The heaviest decrease of river runoff was shown in August under RCP4.5 and in May under the RCP8.5 for the 21st Century in Beas river basin. It indicates that the summer peak flow in Beas river basin will shift to the other seasons. Furthermore, large uncertainties in the study of water future at Beas river basin under climate change can be seen. More importantly, the high resolution WRF precipitation suggested a much higher winter precipitation over high altitude area in in Beas river basin than we knew from the gauge data and other available gridded data set.

#### 400 ACKNOWLEDGMENTS

We are grateful to Dr. W.W. Immerzeel and Dr. A.F. Lutz for providing the ensemble glacier extent data in Upper Indus Basin we used in the study. This study was jointly funded by the Research Council of Norway (RCN) project 216576 (NORINDIA), project- JOINTINDNOR 203867 and project GLACINDIA 033L164.

#### References

- 405 Aggarwal, S.P., Thakur, P.K., Garg, V., Nikam, B.R., Chouksey, A., Dhote, P. and Bhattacharya, T., 2016. WATER RESOURCES STATUS AND AVAILABILITY ASSESSMENT IN CURRENT AND FUTURE CLIMATE CHANGE SCENARIOS FOR BEAS RIVER BASIN OF NORTH WESTERN HIMALAYA. *International Archives of the Photogrammetry, Remote Sensing & Spatial Information Sciences*, 40.
- AKHTAR, M., AHMAD, N. & BOOIJ, M. J. 2008. The impact of climate change on the water resources of Hindukush-Karakorum-Himalaya region under different glacier coverage scenarios. *Journal of Hydrology*, 355, 148-163.
- 410 ALI, D., SACCHETTO, E., DUMONTET, E., LE CARRER, D., ORSONNEAU, J. L., DELAROCHE, O. & BIGOT-CORBEL, E. 2014. Hemolysis influence on twenty-two biochemical parameters measurement. *Annales De Biologie Clinique*, 72, 297-311.
- ALI, S., DAN, L., FU, C. B. & KHAN, F. 2015. Twenty first century climatic and hydrological changes over Upper Indus Basin of Himalayan region of Pakistan. *Environmental Research Letters*, 10.
- 415 Anand, J., Devak, M., Gosain, A. K., Khosa, R., and Dhanya, C. T.: Spatial Extent of Future Changes in the Hydrologic Cycle Components in Ganga Basin using Ranked CORDEX RCMs, *Hydrol. Earth Syst. Sci. Discuss.*, <https://doi.org/10.5194/hess-2017-189>, in review, 2017.
- Azam, M.F., Wagnon, P., Vincent, C., Ramanathan, A., Linda, A. and Singh, V.B., 2014. Reconstruction of the annual mass balance of Chhota Shigri glacier, Western Himalaya, India, since 1969. *Annals of Glaciology*, 55(66), pp.69-80.
- 420 Berthier, E., Arnaud, Y., Kumar, R., Ahmad, S., Wagnon, P. and Chevallier, P., 2007. Remote sensing estimates of glacier mass balances in the Himachal Pradesh (Western Himalaya, India). *Remote Sensing of Environment*, 108(3), pp.327-338.
- Berthier, E. (2006) GLIMS Glacier Database. Boulder, CO: National Snow and Ice Data Center/World Data Center for Glaciology. Digital Media.
- 425 Bolch, T., A. Kulkarni, A. Kääb, C. Huggel, F. Paul, J.G. Cogley, H. Frey, J.S. Kargel, K. Fujita, M. Scheel, S. Bajracharya, M. Stoffel. 2012. The state and fate of Himalayan glaciers. *Science*, 336, pp. 310–314
- Biskop, S., Krause, P., Helmschrot, J., Fink, M., & Flügel, W. A. (2012). Assessment of data uncertainty and plausibility over the Nam Co Region, Tibet. *Advances in Geosciences*, 31, 57-65.



- 430 Chen, H., Xu, C.Y. and Guo, S., 2012. Comparison and evaluation of multiple GCMs, statistical downscaling and hydrological models in the study of climate change impacts on runoff. *Journal of hydrology*, 434, pp.36-45.
- Chen, H., Guo, J., Xiong, W., Guo, S.L., Xu, C.Y., 2010. Downscaling GCMs using the Smooth Support Vector Machine method to predict daily precipitation in the Hanjiang Basin. *Adv. Atmos. Sci.* 27 (2), 274@C284.
- Chu, J. T., Xia J., and Xu C. Y., 2010: Statistical downscaling of daily mean temperature, pan evaporation and precipitation for climate change scenarios in Haihe River, China. *Theor. App. Climatol.*, 99(1-2), 149–161, doi:10.1007/s00704-009-0129-6.
- 435 Collier, E., Mölg, T., Maussion, F., Scherer, D., Mayer, C., & Bush, A. B. G. (2013). High-resolution interactive modelling of the mountain glacier–atmosphere interface: an application over the Karakoram. *The Cryosphere Discussions*, 7(1), 103-144.
- 440 Dee, D. P., Uppala, S. M., Simmons, A. J., Berrisford, P., Poli, P., Kobayashi, S., ... & Vitart, F. (2011). The ERA-Interim reanalysis: Configuration and performance of the data assimilation system. *Quarterly Journal of the Royal Meteorological Society*, 137(656), 553-597.
- Dibike, Y., and Coulibaly P., 2005: Hydrologic impact of climate change in the Saguenay watershed: comparison of downscaling methods and hydrologic models. *J. Hydrol.* 307(1-4), 145–163, doi:10.1016/j.jhydrol.2004.10.012.
- 445 Dimri, A. P., Yasunari, T., Wiltshire, A., Kumar, P., Mathison, C., Ridley, J., and Jacob, D.: Application of regional climate models to the Indian winter monsoon over the western Himalayas, *Sci. Total Environ.*, online first, doi:10.1016/j.scitotenv.2013.01.040, 2013.
- Engelhardt, M., Schuler, T. V. & Andreassen, L. M. (2012) Evaluation of gridded precipitation for Norway using glacier mass-balance measurements. *Geogr. Ann. A* 94, 501–509, doi: 10.1111/j.1468-0459.2012.00473.x.
- 450 ENGELHARDT, M., RAMANATHAN, A., EIDHAMMER, T., KUMAR, P., LANDGREN, O., MANDAL, A. and RASMUSSEN, R., 2017. Modelling 60 years of glacier mass balance and runoff for Chhota Shigri Glacier, Western Himalaya, Northern India. *Journal of Glaciology*, pp.1-11.
- EDEN, J. M., WIDMANN, M., MARAUN, D. & VRAC, M. 2014. Comparison of GCM- and RCM-simulated precipitation following stochastic postprocessing. *Journal of Geophysical Research-Atmospheres*, 119, 11040-11053.
- 455 FUJIHARA, Y., TANAKA, K., WATANABE, T., NAGANO, T. & KOJIRI, T. 2008. Assessing the impacts of climate change on the water resources of the Seyhan River Basin in Turkey: Use of dynamically downscaled data for hydrologic simulations. *Journal of Hydrology*, 353, 33-48.
- GONG, L., WIDEN-NILSSON, E., HALLDIN, S. & XU, C. Y. 2009. Large-scale runoff routing with an aggregated network-response function. *Journal of Hydrology*, 368, 237-250.
- 460 Gong, L., Halldin, S. & Xu, C. Y. (2011) Global scale river routing—an efficient time delay algorithm based on HydroSHEDS high resolution hydrography. *Hydrol. Processes* 25(7), 1114–1128.
- Gemmer, M, Becker S, and Jiang T., 2004: Observed monthly precipitation trends in China 1951@C2002. *Theor. App. Climatol.*, 77(1-2): 39@C45, doi:10.1007/s00704-003-0018-3.
- Hartmann, H. and Andresky, L.: Flooding in the Indus River basin – a spatiotemporal analysis of precipitation records, *Global Planet. Change*, 107, 25–35, doi:10.1016/j.gloplacha.2013.04.002, 2013.
- 465 HASSON, S., LUCARINI, V., KHAN, M. R., PETITTA, M., BOLCH, T. & GIOLI, G. 2014. Early 21st century snow cover state over the western river basins of the Indus River system. *Hydrology and Earth System Sciences*, 18, 4077-4100.
- Hasson, S., 2016. Future Water Availability from Hindukush-Karakoram-Himalaya upper Indus Basin under Conflicting Climate Change Scenarios. *Climate*, 4(3), p.40.
- 470 Hessami M, Gachon P, Ouarda TBMJ, St-Hilaire A. 2008. Automated regression-based statistical downscaling tool. *Environmental Modelling and Software* 23: 813–834.



- Hewitt, K., 2005. The Karakoram anomaly? Glacier expansion and the 'elevation effect', Karakoram Himalaya Mountain Research and Development, 25, pp. 332–340
- Hock, R. (2003) Temperature index modelling in mountain areas. *J. Hydrol.* 282(1–4), 104–115.
- 475 Huffman, G. J., Adler, R. F., Bolvin, D. T., Gu, G., Nelkin, E. J., Bowman, K. P., Hong, Y., Stocker, E. F., and Wolff, D. B.: The TRMM multi-satellite precipitation analysis: Quasi-global, multi-year, combined-sensor precipitation estimates at fine scale, *J. Hydrometeor.*, 8(1), 38–55, 2007.
- HORTON, P., SCHAEFLI, B., MEZGHANI, A., HINGRAY, B. & MUSY, A. 2006. Assessment of climate-change impacts on alpine discharge regimes with climate model uncertainty. *Hydrological Processes*, 20, 2091–2109.
- 480 Immerzeel, W.W., Wanders, N., Lutz, A.F., Shea, J.M. and Bierkens, M.F.P., 2015. Reconciling high-altitude precipitation in the upper Indus basin with glacier mass balances and runoff. *Hydrology and Earth System Sciences*, 19(11), p.4673.
- Immerzeel, W., Pellicciotti, F., and Bierkens, M., (2013). Rising river flows throughout the twenty-first century in two Himalayan glacierized watersheds, *Nat. Geosci.*, 6, 742–745, doi:10.1038/NGEO1896, 4757, 4761, 4773.
- Jacob D, et al (2014) EURO-CORDEX: new high-resolution climate change projections for European impact research. *Reg*
- 485 *Environ Chang* 14(2):563–578. doi:10.1007/s10113-013-0499-2.
- Ji, ZM. and Kang, SC., 2015. Evaluation of extreme climate events using a regional climate model for China. *International Journal of Climatology*, 35(6), pp.888–902.
- Ji ZM, Kang SC, 2013. Projection of snow cover changes over China under RCP scenarios. *Climate Dynamics*, 41, 589–600.
- JOHNSON, F. & SHARMA, A. 2015. What are the impacts of bias correction on future drought projections? *Journal of*
- 490 *Hydrology*, 525, 472–485.
- Kääb, A., Treichler, D., Nuth, C. and Berthier, E., 2015. Brief Communication: Contending estimates of 2003–2008 glacier mass balance over the Pamir–Karakoram–Himalaya. *The Cryosphere*, 9(2), pp.557–564.
- Koukidis, E. N., and Berg, 2009: Sensitivity of the statistical downscaling model (sds) to reanalysis products. *Atmos. Ocean*, 47(1): 1–18, doi:10.3137/AO924.2009.
- 495 KHAN, F., PILZ, J., AMJAD, M. & WIBERG, D. A. 2015. Climate variability and its impacts on water resources in the Upper Indus Basin under IPCC climate change scenarios. *International Journal of Global Warming*, 8, 46–69.
- KUMAR, V., SINGH, P. & SINGH, V. 2007a. Snow and glacier melt contribution in the Beas River at Pandoh Dam, Himachal Pradesh, India. *Hydrological sciences journal*, 52, 376–388.
- KUMAR, V., SINGH, P. & SINGH, V. 2007b. Snow and glacier melt contribution in the Beas River at Pandoh Dam, Himachal Pradesh, India. *Hydrological Sciences Journal-Journal Des Sciences Hydrologiques*, 52, 376–388.
- 500 Lee, Y. J., and Mangasarian, O. L. (2001). SSVM: a smooth support vector machine for classification. *Computational Optimization & Applications*, 20(1), 5–22.
- Li, L., Engelhard M., Xu, C.Y., JAIN, S.J., Singh, V.P., 2013a. Comparison of satellite-based and reanalysed precipitation as input to glacio-hydrological modeling for Beas river basin, Northern India. *Cold and Mountain Region Hydrological*
- 505 *Systems Under Climate Change: Towards Improved Projections*. IAHS Publ. 360. 45–52.
- Li, L., Ngongondo, C. S., Xu, C. Y., & Gong, L. 2013b. Comparison of the global TRMM and WFD precipitation datasets in driving a large-scale hydrological model in Southern Africa. *Hydrol Res.* doi, 10, 2166.
- Li H, Xu C-Y, Beldring S, Tallaksen TM, Jain SK, 2016. Water Resources under Climate Change in Himalayan basins. *Water Resources Management* 30:843–859. DOI:10.1007/s11269-015-1194-5.
- 510 Li, H, Beldring S, Xu\* C-Y, Huss M, Melvold K, 2015a. Integrating a glacier retreat model into a hydrological model -- case studies on three glacierised catchments in Norway and Himalayan region. *Journal of Hydrology* 527, 656–667. doi:10.1016/j.jhydrol.2015.05.017.



- Li L, Diallo I, Xu C-Y, Stordal F, 2015b. Hydrological projections under climate change in the near future by RegCM4 in Southern Africa using a large-scale hydrological model. *Journal of Hydrology* 528, 1-16,  
515 doi:10.1016/j.jhydrol.2015.05.028.
- Li, L., Gochis, D.J., Sobolowski, S. and Mesquita, M.D., 2017. Evaluating the present annual water budget of a Himalayan headwater river basin using a high-resolution atmosphere-hydrology model. *Journal of Geophysical Research: Atmospheres*, 122(9), pp.4786-4807.
- LUTZ, A. F., IMMERZEEL, W. W., KRAAIJENBRINK, P. D. A., SHRESTHA, A. B. & BIERKENS, M. F. P. 2016. Climate Change Impacts on the Upper Indus Hydrology: Sources, Shifts and Extremes. *Plos One*, 11.  
520
- LUTZ, A. F., IMMERZEEL, W. W., SHRESTHA, A. B. & BIERKENS, M. F. P. 2014. Consistent increase in High Asia's runoff due to increasing glacier melt and precipitation. *Nature Climate Change*, 4, 587-592.
- MAUSSION, F., SCHERER, D., FINKELNBURG, R., RICHTERS, J., YANG, W. & YAO, T. 2011. WRF simulation of a precipitation event over the Tibetan Plateau, China - an assessment using remote sensing and ground observations.  
525 *Hydrology and Earth System Sciences*, 15, 1795-1817.
- Mair, E., Bertoldi, G., Leitinger, G., Chiesa, S. D., Niedrist, G., & Tappeiner, U. (2013). ESOLIP—estimate of solid and liquid precipitation at sub-daily time resolution by combining snow height and rain gauge measurements. *Hydrology and Earth System Sciences Discussions*, 10(7), 8683-8714.
- Ménégoz, M., Gallée, H., & Jacobi, H. W. (2013). Precipitation and snow cover in the Himalaya: from reanalysis to regional  
530 climate simulations. *Hydrology and Earth System Sciences*, 17(10), 3921-3936.
- Mishra, V., 2015. Climatic uncertainty in Himalayan water towers. *Journal of Geophysical Research: Atmospheres*, 120(7), pp.2689-2705.
- Mitchell, T. D. and Jones, P. D.: An improved method of constructing a database of monthly climate observations and associated high-resolution grids, *Int. J. Climatol.*, 25, 693–712, 2005.
- 535 Rasmussen, R., Liu, C., Ikeda, K., Gochis, D., Yates, D., Chen, F., ... & Gutmann, E., 2011. High-resolution coupled climate runoff simulations of seasonal snowfall over Colorado: a process study of current and warmer climate. *Journal of Climate*, 24(12), 3015-3048. doi: <http://dx.doi.org/10.1175/2010JCLI3985.1>
- Rasmussen, R.M., K. Ikeda, C. Liu, D.J. Gochis, M. Clark, A. Dai, E. Gutmann, J. Dudhia, F. Chen, M.J. Barlage, D. Yates, and G. Zhang, 2014: Climate change impacts on the water balance of the Colorado headwaters: High-resolution regional  
540 climate model simulations. *Journal of Hydrometeorology*, 15, 1091-1116, DOI: 10.1175/JHM-D-13-0118.1.
- Raup, B. H., Racoviteanu, A., Khalsa, S. J. S., Helm, C., Armstrong, R. & Arnaud Y. (2007) The GLIMS Geospatial Glacier Database: a new tool for studying glacier change. *Global Planetary Change* 56, 101–110. (doi:10.1016/j.gloplacha.2006.07.018).
- Ragettli, S. and Pellicciotti, F. (2012). Calibration of a physically based, spatially distributed hydrological model in a  
545 glacierized basin: on the use of knowledge from glaciometeorological processes to constrain model parameters, *Water Resour. Res.*, 48, 1–20, doi:10.1029/2011WR010559, 4757
- Rudd, A.C., A. L. and Kay, 2016: Use of very high resolution climate model data for hydrological modelling: estimation of potential evaporation. *Hydrol. Res.*, 47(3), 660-670, doi:10.2166/nh.2015.028.
- Singh, S., S. Ghosh, A. S. Sahana, H. Vittal, and S. Karmakar, 2017: Do dynamic regional models add value to the global  
550 model projections of Indian monsoon? *Clim Dyn*, 48, 1375–1397, doi:10.1007/s00382-016-3147-y.
- Shrestha, M., Wang, L., Koike, T., Xue, Y., and Hirabayashi, Y.: Modeling the spatial distribution of snow cover in the Dudhkoshi Region of the Nepal Himalayas, *J. Hydrometeorol.*, 13, 204–222, doi:10.1175/JHM-D-10-05027.1, 2012
- STAHL, K., MOORE, R. D., SHEA, J. M., HUTCHINSON, D. & CANNON, A. J. 2008. Coupled modelling of glacier and streamflow response to future climate scenarios. *Water Resources Research*, 44.



- 555 Tatsumi, K., T. Oizumi, and Y. Yamashiki, 2014: Assessment of future precipitation indices in the Shikoku region using a statistical downscaling model. *Stoch. Env. Res. Risk A.*, 28(6), 1447–1464, doi:10.1007/s00477-014-0847-x.
- Taylor, K. E., R. J. Stouffer, and G. A. Meehl, 2012: An overview of CMIP5 and the experiment design. *B. Am. Meteorol. Soc.*, 93(4), 485-498, doi:10.1175/BAMS-D-11-00094.1.
- TEUTSCHBEIN, C. & SEIBERT, J. 2012. Bias correction of regional climate model simulations for hydrological climate-change impact studies: Review and evaluation of different methods. *Journal of Hydrology*, 456, 12-29.
- 560 TROIN, M., VELAZQUEZ, J. A., CAYA, D. & BRISSETTE, F. 2015. Comparing statistical post-processing of regional and global climate scenarios for hydrological impacts assessment: A case study of two Canadian catchments. *Journal of Hydrology*, 520, 268-288.
- Vapnik, V. N., 1998: *Statistical Learning Theory*. Wiley. New York.
- 565 Vincent, C., Ramanathan, A., Wagnon, P., Dobhal, D.P., Linda, A., Berthier, E., Sharma, P., Arnaud, Y., Azam, M.F. and Gardelle, J., 2013. Balanced conditions or slight mass gain of glaciers in the Lahaul and Spiti region (northern India, Himalaya) during the nineties preceded recent mass loss. *The Cryosphere*, 7(2), pp.569-582.
- Vuuren, D. P. V., and Coauthors, 2011: The representative concentration pathways: an overview. *Climatic Change*, 109(1-2), 5-31, doi:10.1007/s10584-011-0148-z.
- 570 WIDEN-NILSSON, E., GONG, L., HALLDIN, S. & XU, C. Y. 2009. Model performance and parameter behavior for varying time aggregations and evaluation criteria in the WASMOD-M global water balance model. *Water Resources Research*, 45.
- WILBY, R. L., DAWSON, C. W. & BARROW, E. M. 2002. SDSM - a decision support tool for the assessment of regional climate change impacts. *Environmental Modelling & Software*, 17, 147-159.
- 575 Wilby, R. L., and C. W. Dawson, 2013: The statistical downscaling model: insights from one decade of application. *Int. J. Climatol.*, 33(7), 1707–1719, doi:10.1002/joc.3544.
- Wilby, R. L., and C. W. Dawson, 2013: The statistical downscaling model: insights from one decade of application. *Int. J. Climatol.*, 33(7), 1707@C1719, doi:10.1002/joc.3544.
- Wilby R L, Dawson C W, Barrow E M. 2002, SDSM - a decision support tool for the assessment of regional climate change
- 580 impacts. *Environmental Modelling & Software*, 17(2):145-157.
- Winiger, M. G. H. Y., Gumpert, M., & Yamout, H. (2005). Karakorum–Hindukush–western Himalaya: assessing high-altitude water resources. *Hydrological Processes*, 19(12), 2329-2338.
- XU, C.-Y. 2002. WASMOD - The Water And Snow balance MODelling system. In: SINGH, V. P. & FREVERT, D. K. (eds.) *Mathematical Models of Small Watershed Hydrology and Applications*. LLC, Chelsea, Michigan, USA: Water
- 585 Resources Publications.
- Yatagai, A. et al (2012): PHRODITE: Constructing a Long-Term Daily Gridded Precipitation Dataset for Asia Based on a Dense Network of Rain Gauges. *Bull. Amer. Meteor. Soc.*, 93, 1401-1415.



Table 1. Daily GSM-WASMOD variables and their equations

Variable controlled	Parameter (units)	Equation
<b>WASMOD-D module</b>		
Snow fall	$a_1, a_2$ (°C)	$s_t = p_t \left\{ 1 - \exp\left(-\left(\frac{T_a - a_1}{a_1 - a_2}\right)^2\right)\right\}^t$ (1)
Rainfall		$r_t = p_t - s_t$ (2)
Snow storage		$sp_t = sp_{t-1} + s_t - m_t$ (3)
Snow melt		$m_t = sp_t \cdot \left\{ 1 - \exp\left(-\left(\frac{a_2 - T_a}{a_1 - a_2}\right)^2\right)\right\}^t$ (4)
Actual evapotranspiration	$a_4$ (-)	$e_t = \min[ep_t(1 - a_4^{w_t/ep_t}), w_t]$ (5)
Available water		$w_t = r_t + sm_{t-1}^+$ (6)
Saturated percentage area	$c_1$ (-)	$sp_t = 1 - e^{-c_1 w_t}$ (7)
Fast flow		$s_t = (r_t + m_t) \cdot sp_t$ (8)
Slow flow	$c_2$ (mm <sup>-1</sup> day)	$f_t = w_t \left(1 - e^{-c_2 w_t}\right)$ (9)
Total flow		$d_t = s_t + f_t$ (10)
Land moisture		$sm_t = sm_{t-1} + r_t + m_t - e_t - d_t$ (11)
<b>Glacier and snow (GSM) module</b>		
Glacier and snow mass gain	$T_a$ (°C), $\Delta T$ (K)	$G_t = \begin{cases} p_t & \forall T_a \leq T_s - \Delta T / 2 \\ p_t \cdot [(T_s - T_a) / \Delta T + 0.5] & \forall T_s - \Delta T / 2 < T_a < T_s + \Delta T / 2 \\ 0 & \forall T_a \geq T_s + \Delta T / 2 \end{cases}$ (12)
Glacier and snow mass melt	$DDF$	$M_t = DDF(T_a - T_0)$ (13)

where  $\{x\}^+$  means  $\max(x, 0)$  and  $\{x\}^-$  means  $\min(x, 0)$ ;  $ep_t$  is the daily potential evapotranspiration;  $a_1$  is the snowfall temperature and

590  $a_2$  is the snow melt temperature;  $T_a$  is air temperature (°C);  $p_t$  is the precipitation in a given day;  $sm_{t-1}$  is the land moisture (a available storage;  $T_s$  is a threshold temperature for snow distinguishes between rain and snow  $T_s = 1$  °C;  $\Delta T$  is a temperature interval,  $\Delta T = 2$  K;  $DDF$  is the degree day factor and  $T_0$  is the melt threshold factor in GSM module.





595 Table 2. The GCMs and RCPs for ensemble for glacier revolution simulations.

Description	RCPs	Selected model
Dry&Cold	RCP4.5	Inmem4_r1ip1
Dry&Warm	RCP4.5	IPSL-CM5A-LR_r3ip1
Wet&Warm	RCP4.5	MRI_CGCM3_r1i1p1
Wet&Cold	RCP4.5	CamESM2_r4i1p1
Dry&Cold	RCP8.5	MPI-ESM-LR_r1i1p1
Dry&Warm	RCP8.5	IPSL-CM5A-LR_r3i1p1
Wet&Cold	RCP8.5	CSIRO-Mk3-0_r1i1p1
Wet&Warm	RCP8.5	MIROC5_r3i1p1

*(from Lutz et al., 2014)*



Table3. Calibration (1990-2000) and alidation (2001-2004) of GSM-WASMOD.

Models	Calibration (1990-2000)				Validation (2001-2004)			
	NS_d	NS_m	VE	RMSE	Ns_d	NS_m	VE	RMSE
WASMOD	0.52	0.69	3%	1.0	0.43	0.63	16%	1.29
GSM-WASMOD	0.66	0.74	9%	1.37	0.72	0.79	9%	0.86

*NS\_d: daily Nash-Sutcliffe efficient; NS\_m: monthly Nash-Sutcliffe efficient*



Table 4: Climate change ensemble for GSM-WASMOD at 21st century (2006-2099)

index	RCMs	RCP	Glacier - GCM
0	mean	mean	mean
1	SDSM	45	CamESM2_r4i1p1
2	SDSM	85	CSIRO_Mk3_6_0
3	SVM	45	CamESM2_r4i1p1
4	SVM	85	CSIRO_Mk3_6_0
5	SDSM	45	Inmcm4_r1ip1
6	SDSM	85	IPSL_CM5A_LR
7	SVM	45	Inmcm4_r1ip1
8	SVM	85	IPSL_CM5A_LR
9	SDSM	45	IPSL-CM5A-LR_r3ip1
10	SDSM	85	MIROC5
11	SVM	45	IPSL-CM5A-LR_r3ip1
12	SVM	85	MIROC5
13	SDSM	45	MRI_CGCM3
14	SDSM	85	MRI_ESM_LR
15	SVM	45	MRI_CGCM3
16	SVM	85	MRI_ESM_LR

*CMIP5: Bcc-csm*



Table 5. Annual mean Change

<b>Period</b>	<b>RCP</b>	<b>Glacier cover loss (%)</b>	<b>dP (%)</b>	<b>dT (°C)</b>	<b>dET (%)</b>	<b>dQ (%)</b>
2046-2055	RCP4.5	44(29.7/55.5)	0.5(-0.2/1.2)	0.95(0.58/1.3)	11 (3/16)	-35(-17/-46)
	RCP8.5	48.9(45.4/55.1)	8.8(1.8/15.7)	1.67(0.94/2.4)	17(15/20)	-38(-30/-48)
2090-2099	RCP4.5	72.7(58.4/84.6)	0.8(-1.7/3.4)	1.53(0.95/2.1)	17(14/19)	-49(-48/-50)
	RCP8.5	87.3(84.8/90.5)	6.0(-2.6/14.7)	3.5 (1.5 /5.4)	19(12/24)	-48(-41/-55)

*dP: the changes of precipitation; dT: the changes of temperature; dET: the changes of ET; dQ: the changes of runoff*

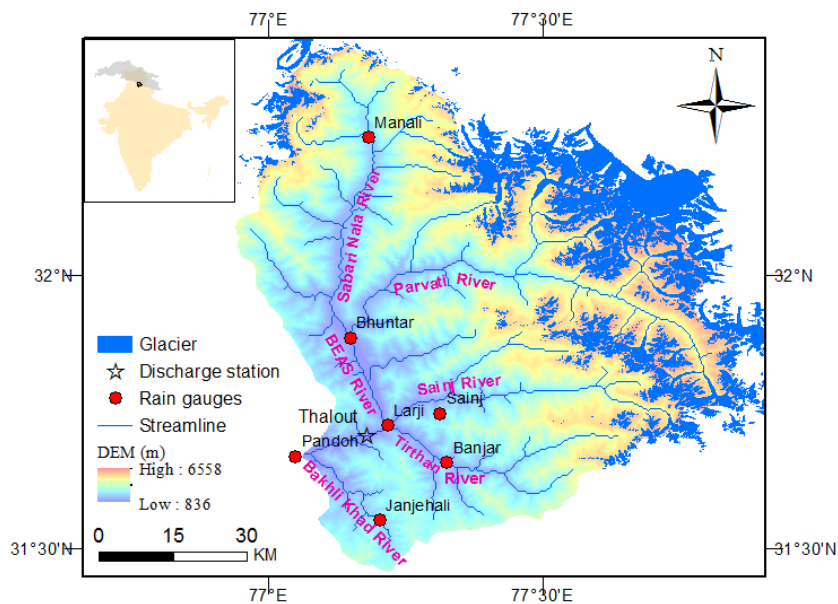
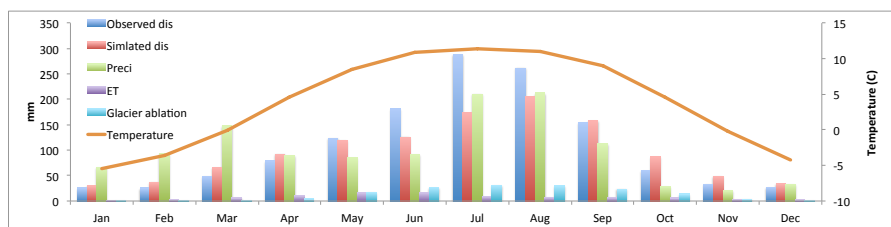


Fig. 1: The topography, stream network and glacier cover of Beas river basin up to Pandoh dam with seven rain gauges and Thalout discharge station (The small figure on the upper right corner shows the location of Beas river basin up to Pandoh within Upper Indus Basin (UIB) region and India).

615



**Fig. 2** Monthly mean of the main water balance terms and observed discharge for the Beas river basin (1990-2004), which shows simulated discharge (Simulated dis), precipitation (Preci), evapotranspiration (ET), Glacier ablation (in the primary axis on the left side) and temperature (in the secondary axis on right side).

620



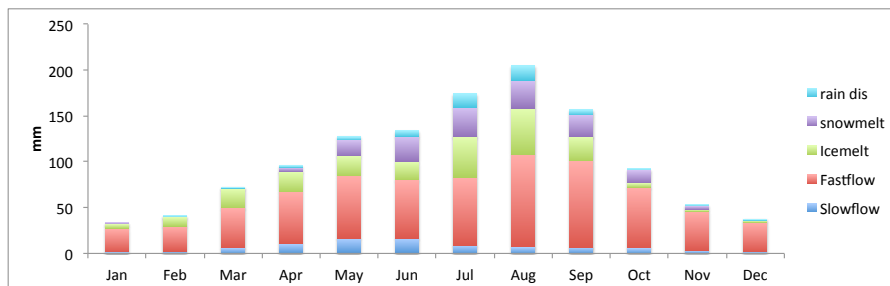
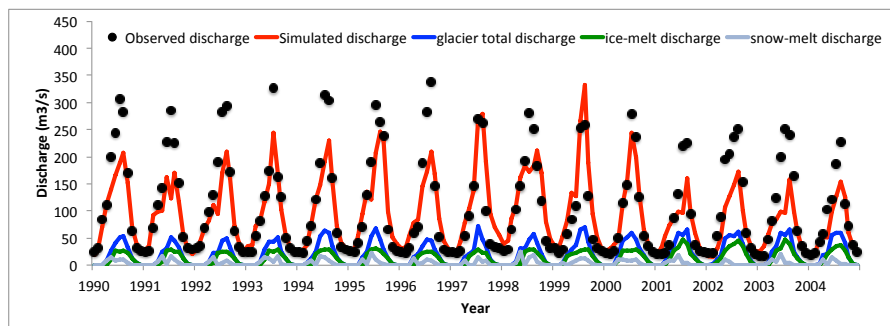
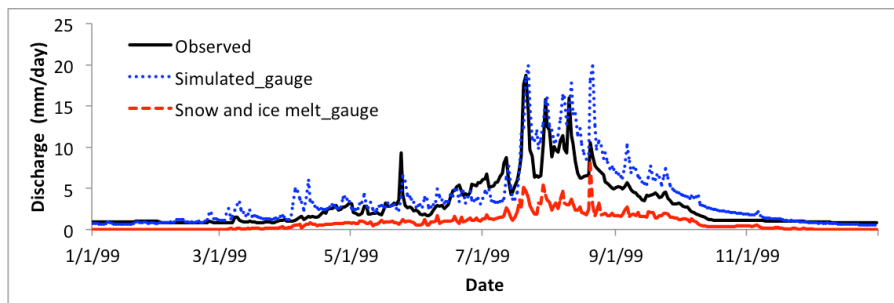


**Fig. 3** Monthly mean of the components of total discharge of Beas river basin (1990-2004), including fast flow, slow flow from non-glacier area and discharges from glacier area, which includes rainfall discharge (rain dis), snow-melt and ice-melt discharge.



625

Fig. 4 Monthly hydrography of the observed (dots) and simulated discharge (red line), total discharge from glacier (blue line), ice melting (green line) and snow melting discharge (gray line) in Beas river basin up to Thalout during 1990-2004.



630 Fig. 5 The daily observed and simulated Discharge, snow and ice melt runoff in Beas river basin at 1999.

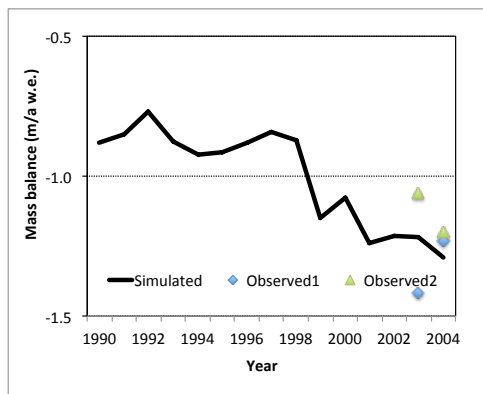
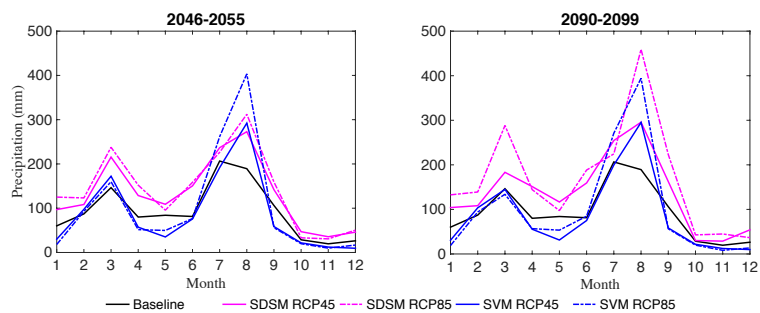
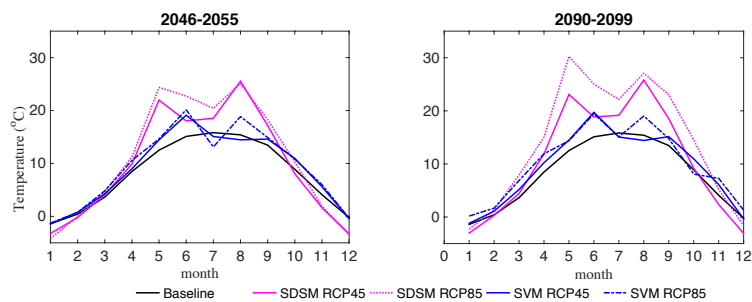


Fig. 6 Simulated and observed (Observed 1 (Azam et al., 2016) and Observed2 (Vincent et al., 2013)) annual glacier mass balance of Beas River basin (mainly from Chhota Shigri) from 1990-2004.

635

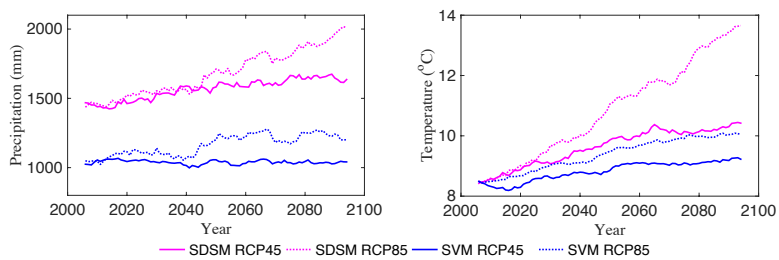


**Fig. 7** Average monthly mean observed (Baseline) and simulated precipitations for the two RCMs with RCP4.5 and RCP8.5 for (a) 2046-2055, (b) 2090-2099 over Beas river basin.



640 **Fig. 8** Average monthly mean observed (Baseline) and simulated temperature for the two RCMs with RCP4.5 and RCP8.5 for (a) 2046-2055, (b) 2090-2099 over Beas river basin.





645 **Fig. 9** Ten-yr's moving average of annual precipitation and temperature of the Beas river basin.

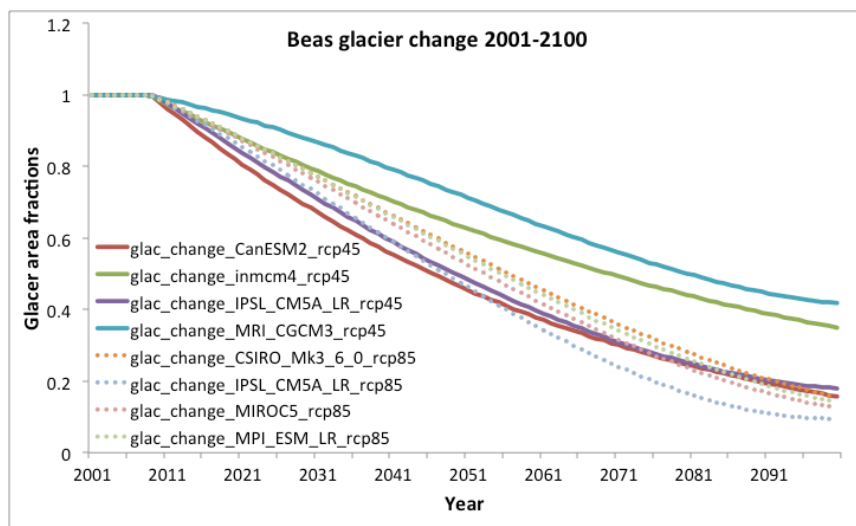
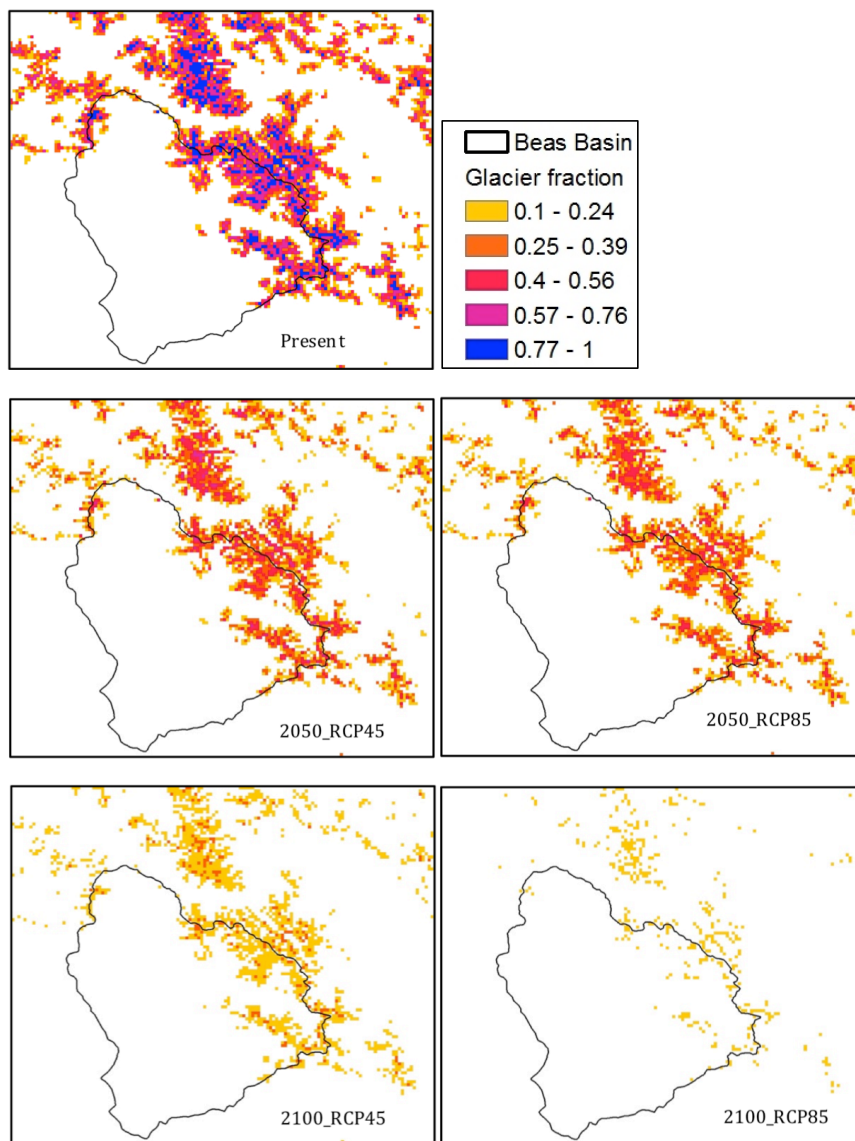


Fig. 10 Projected changes in glacier extent for Beas river basin during 21st century.



650



655 Fig. 11 Glacier fraction change 2001-2100 (note: 2050 RCP4.5:0.57725, RCP8.5: 0.53375; 2100 RCP4.5:0.27575, RCP8.5: 0.1295).

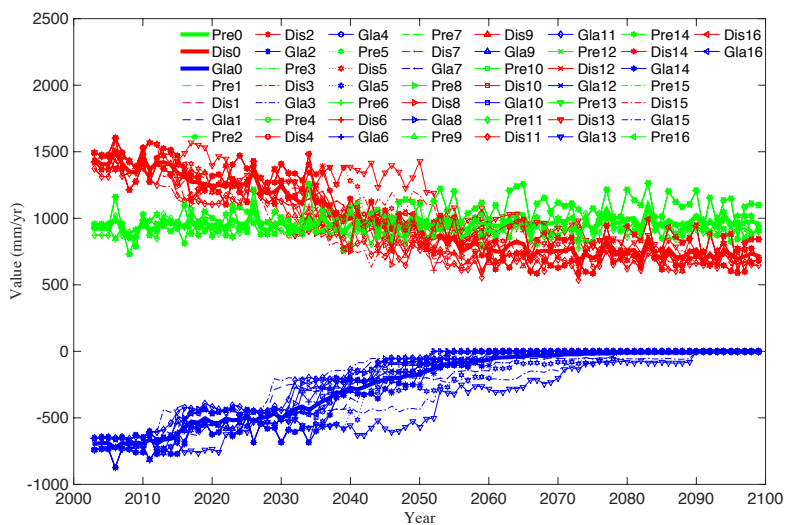


**Fig. 12** Annual precipitation, total discharge and glacier-melt discharge under Climate change (from CANESM2) RCP4.5 and RCP8.5 from 2005 to 2099 (the tipping point year is 2026 and 2052).



660

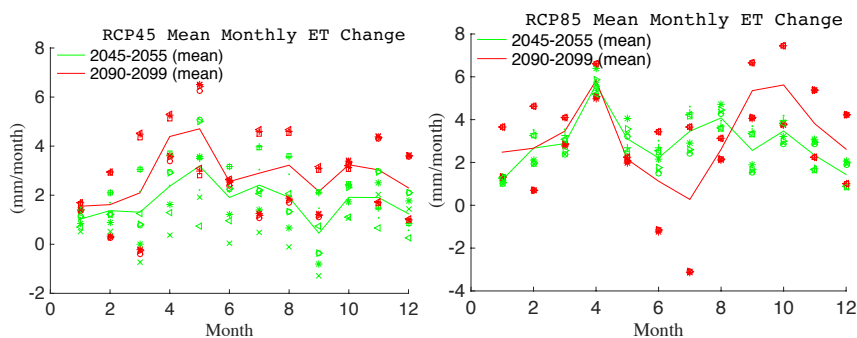


**Fig. 13** mean monthly changes in evapotranspiration (ET) at Beas river basin up to Pandoh. Changes are shown for the middle of the century (2045-2055) and by the end of the century (2090-2099) compared to baseline period (2006-2015) for the RCP4.5 and RCP8.5 scenarios.

665

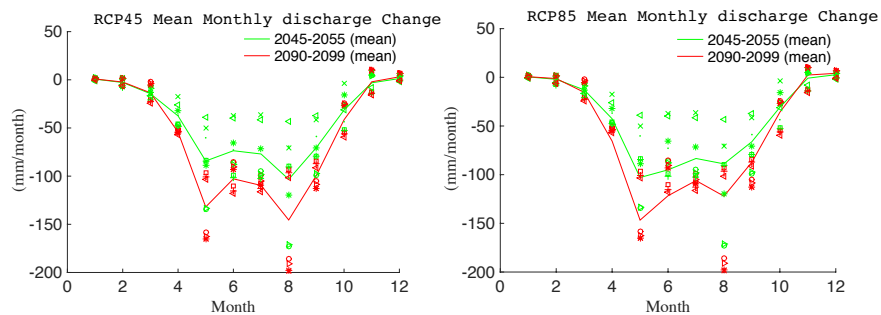


**Fig. 14** mean monthly changes in discharge at Beas river basin up to Pandoh. Changes are shown for the middle of the century (2045-2055) and by the end of the century (2090-2099) compared to baseline period (2006-2015) for the RCP4.5 and RCP8.5 scenarios.

670

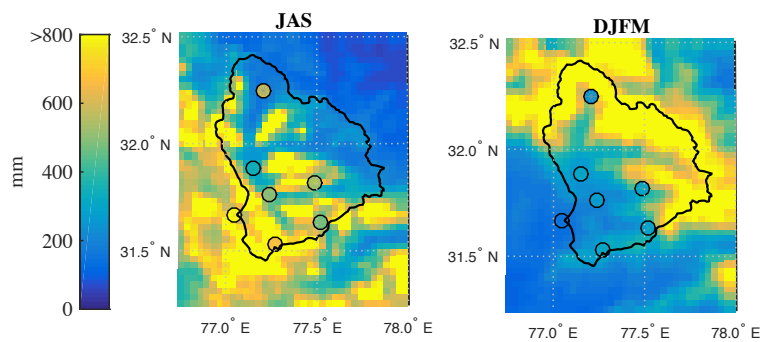


**Fig. 15** Seasonal precipitation (1998-2005) from 3km WRF (from Li et al.(2017)) and Gauge (dot) in Beas River basin. (from Li et al. 2017)



675

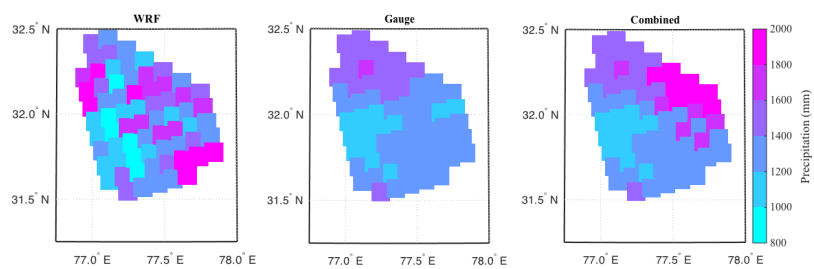


**Fig. 16** Mean annual precipitation from gauge (1316 mm / yr), WRF (1396 mm / yr) and combined precipitation (1413 mm / yr) in Beas river basin of calibration period (1996-2003).